Electronic Supplementary Information: Peculiar anharmonicity of Ruddlesden Popper metal halides: Temperature-dependent phonon dephasing

Esteban Rojas-Gatjens[a], Carlos Silva-Acuña[‡a,b,c], and Ajay Ram Srimath Kandada[d]

[a] *School of Chemistry and Biochemistry, Georgia Institute of Technology, 901 Atlantic Drive, Atlanta, Georgia 30332, United States.*

[b] *School of Physics, Georgia Institute of Technology, 837 State Street, Atlanta, Georgia 30332, United States.*

[c] *School of Materials Science and Engineering, Georgia Institute of Technology, North Avenue, Atlanta, GA 30332, United States. E-mail: carlos.silva@gatech.edu*

[d] *Department of Physics and Center for Functional Materials, Wake Forest University, 1834 Wake Forest Road, Winston-Salem, NC 27109, United States; E-mail: srimatar@wfu.edu*

‡ *Currently visiting as Honorary Professor, Departamento de Física Aplicada, Centro de Investigación y de Estudios Avanzados del Instituto Politécnico Nacional, 97310 Mérida, Yucatán, México.*

1 Methods

The experimental data for the analysis in this work was extracted from Ref. 18. The RISRS experiment was performed in a pump-probe transmission geometry. The data was acquired using a pump photon energy of 3.06 eV, average power of 300 μW at a pulse repetition rate of 100 kHz, focused to a 1.9-mm spot diameter. The oscillatory component of the transient absorption signal between the energies 2.34 and 2.40 eV was binned to generate Fig. 1(b). Experimental details for the RISRS experiment can be found in Ref. 18.

2 Temperature dependent resonant impulsive stimulated Raman Spectra

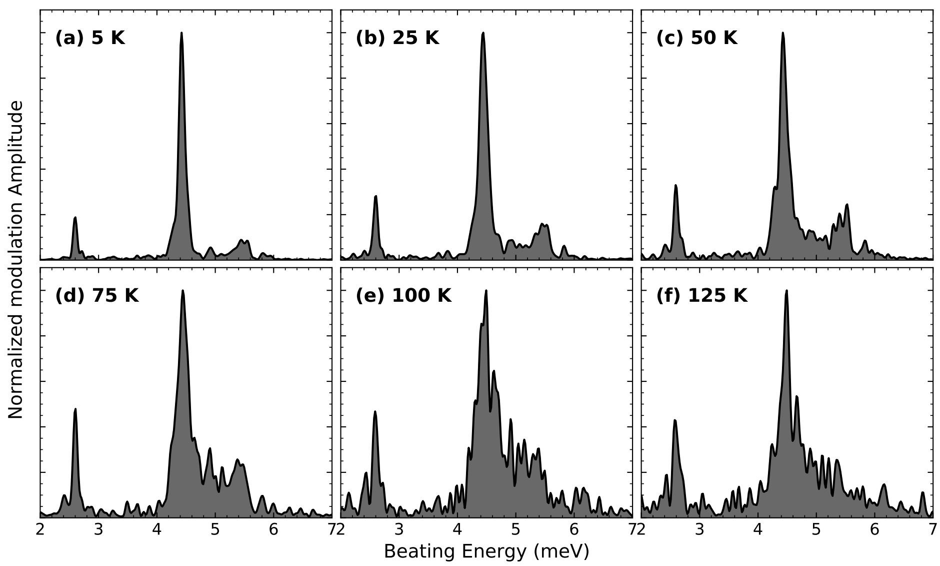

Figure S1: Temperature dependence of the RISRS Spectra for $(PEA)_2PbI_4$.

3 Continuous Wavelet transform (CWT) analysis

The CWT was implemented using the open source wavelet transform software for Python under MIT license[27]. A complex Morlet wavelet was employed for the analysis, equation S1, with parameters B and C equal to 50 and 1 respectively. The wavelet transform is defined as equation S2, were $W(\tau, s)$ are the wavelet coefficients. It can be noted that if $f(t)$ corresponds to a damped oscillation the $|W(\tau, s)|$ will not have an oscillatory component in τ.

$$\psi\left(t\right) = \exp\left(-\frac{t^2}{B}\right) \exp\left(i2\pi Ct\right) \tag{S1}$$

$$W(\tau, s) = \frac{1}{|s|^{1/2}} \int_{-\infty}^{\infty} f\left(t\right)\, \psi^*\left(\frac{t-\tau}{s}\right)\, dt \tag{S2}$$

Using $f(t) = A\,\exp(-\tau/\tau_c)\cos(\omega t + \phi)$ and rearranging equation S2, we obtained expression S3. With a value of B chosen such that $s^2\,B/2\tau_c > \tau$ the influence of τ in the integral is negligible. By taking the norm the dephasing rate is isolated since the complex phase cancels out and we can bin all the τ independent terms together as it is shown in equation S4.

$$W(\tau, s) = \frac{A\, e^{\frac{-s^4 B^2}{4\tau_c}}}{|s|^{1/2}} \left[\int_{-\infty}^{\infty} \cos(\omega t + \phi)\, e^{-\frac{1}{B}\left[t-\left(\tau-\frac{s^2\,B}{2\tau_c}\right)^2\right]} e^{i2\pi Ct/s} dt\right] e^{-i2\pi C\tau/s} e^{-\tau/\tau_c} \tag{S3}$$

$$|W(\tau, s)| \approx |w(s)|\, \exp(-\tau/\tau_c) \tag{S4}$$

3.1 Complete CWT data set

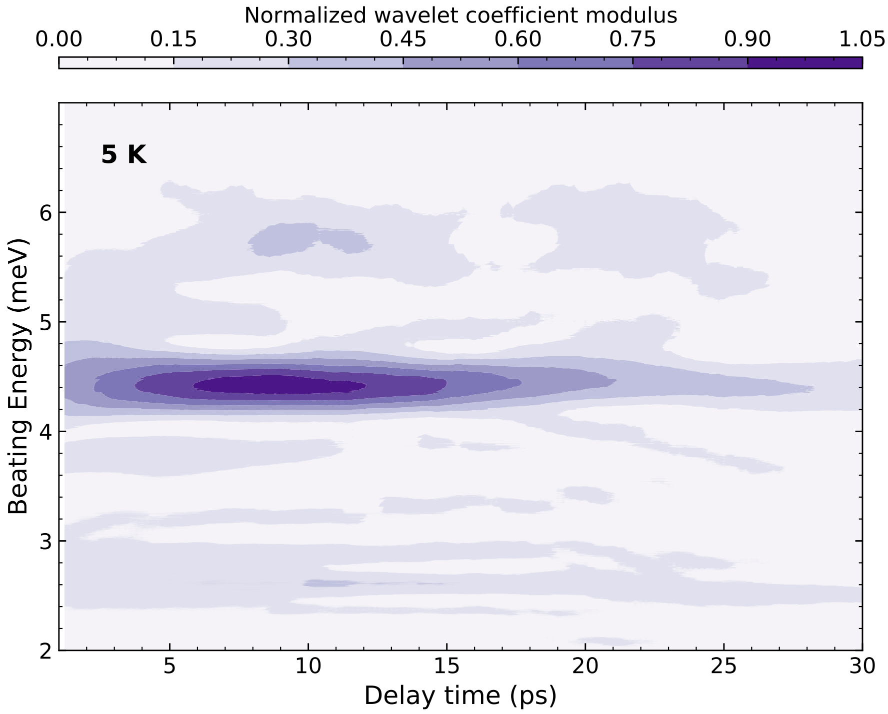

Figure S2: Wavelet transformation (CWT) spectrum of the time-domain RISRS data with a complex Morlet wavelet at 5 K.

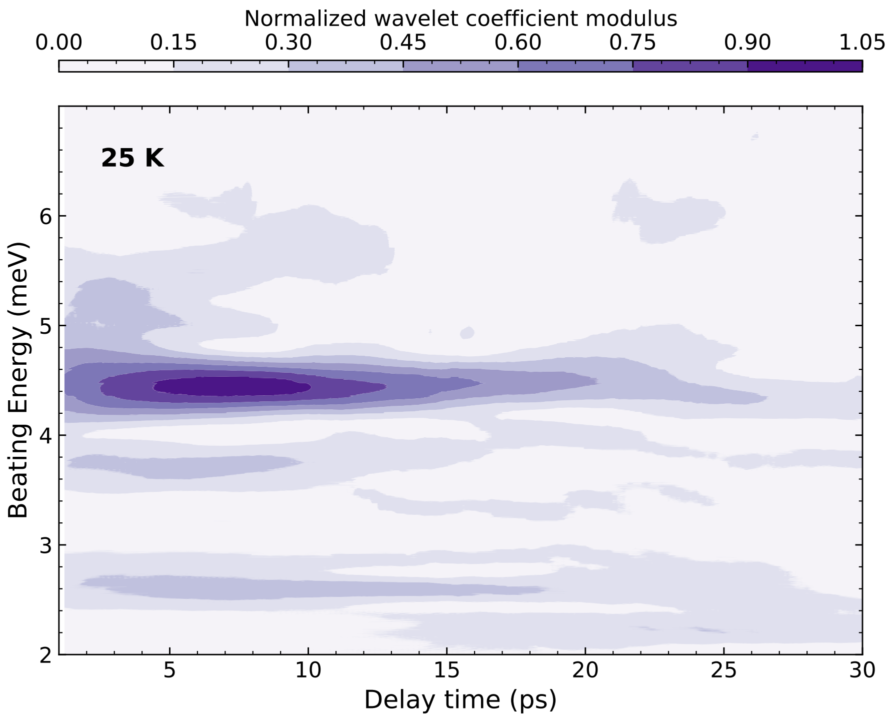

Figure S3: Wavelet transformation (CWT) spectrum of the time-domain RISRS data with a complex Morlet wavelet at 25 K.

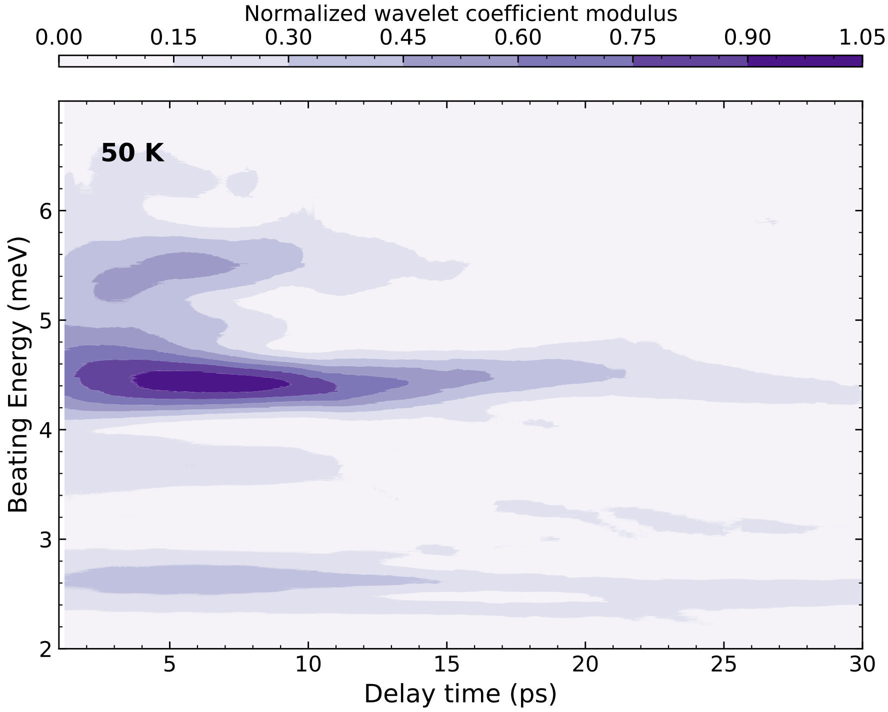

Figure S4: Wavelet transformation (CWT) spectrum of the time-domain RISRS data with a complex Morlet wavelet at 50 K.

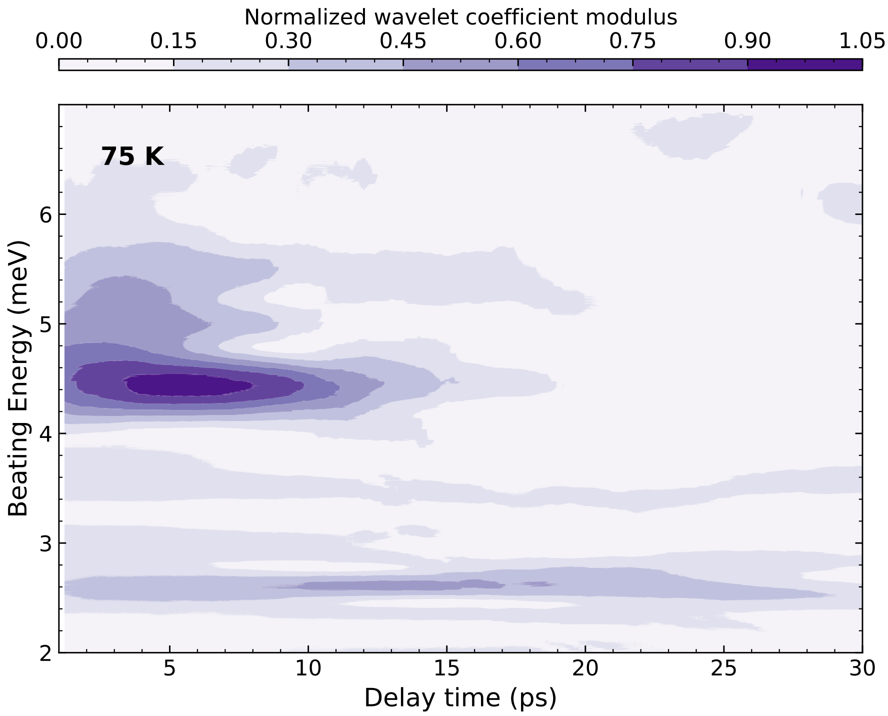

Figure S5: Wavelet transformation (CWT) spectrum of the time-domain RISRS data with a complex Morlet wavelet at 75 K.

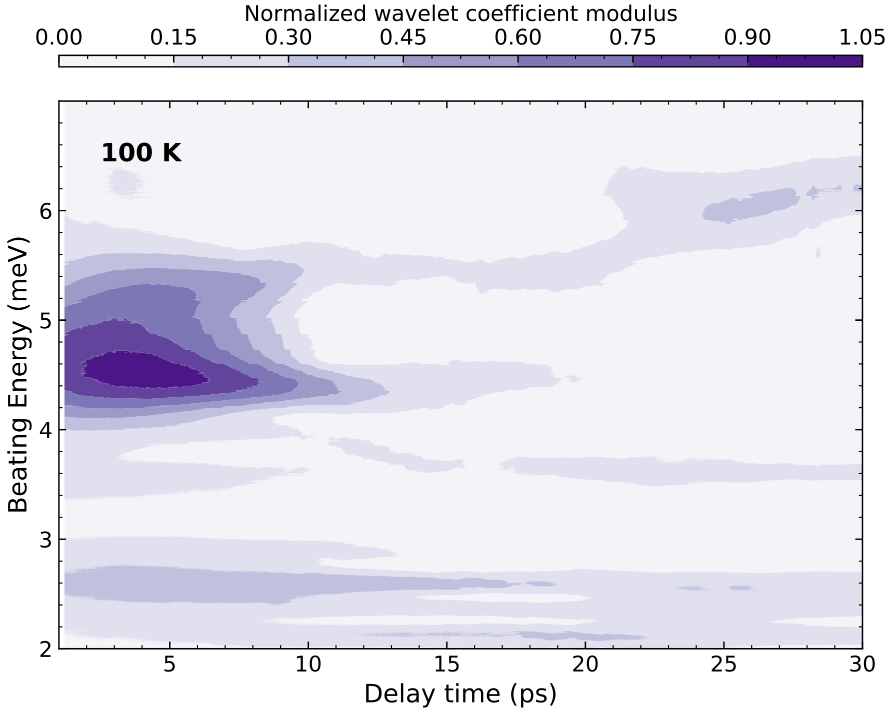

Figure S6: Wavelet transformation (CWT) spectrum of the time-domain RISRS data with a complex Morlet wavelet at 100 K.

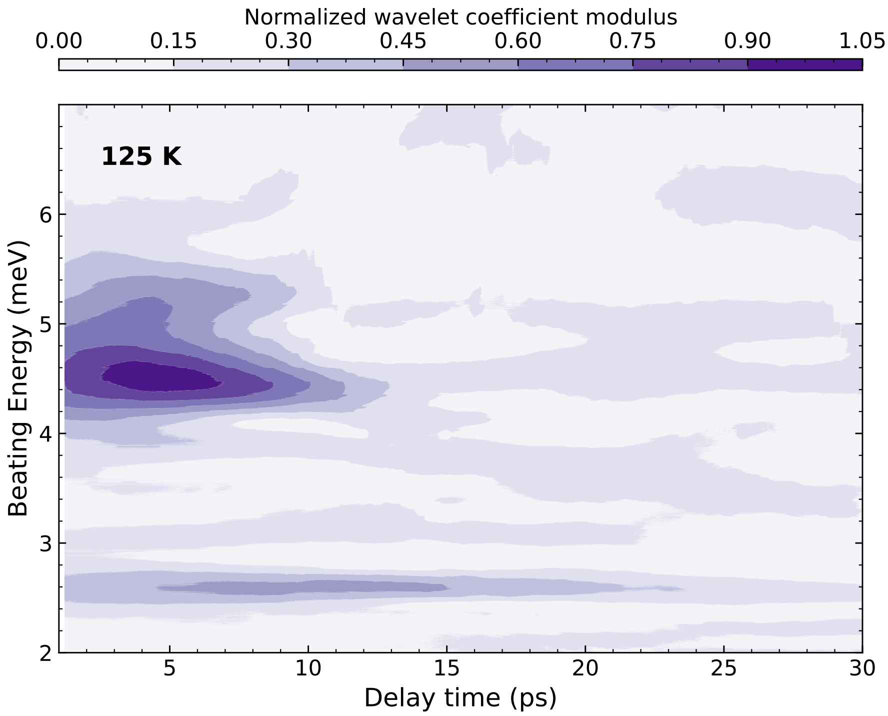

Figure S7: Wavelet transformation (CWT) spectrum of the time-domain RISRS data with a complex Morlet wavelet at 125 K.

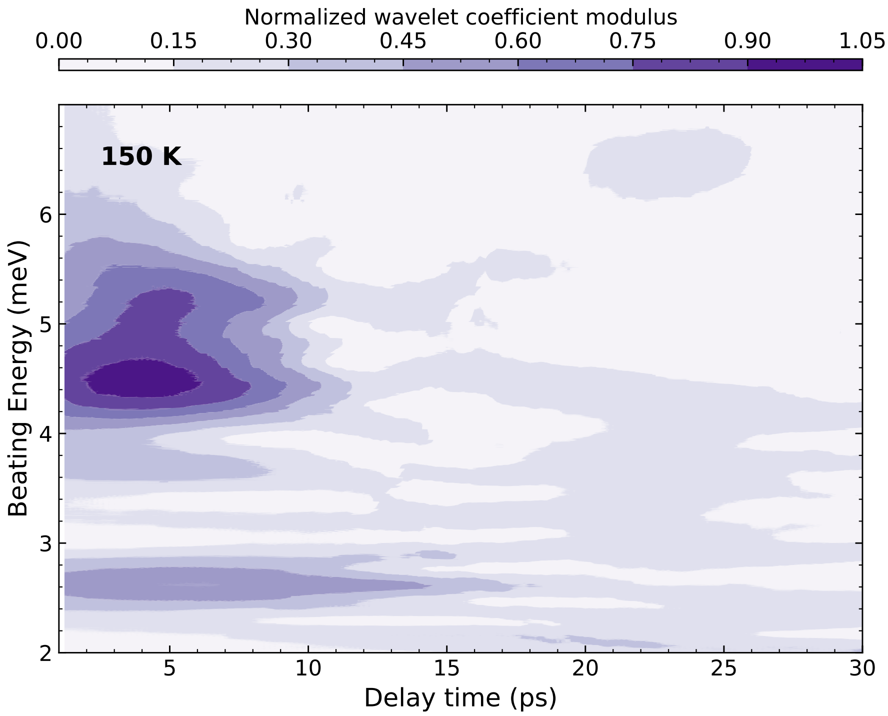

Figure S8: Wavelet transformation (CWT) spectrum of the time-domain RISRS data with a complex Morlet wavelet at 150 K.

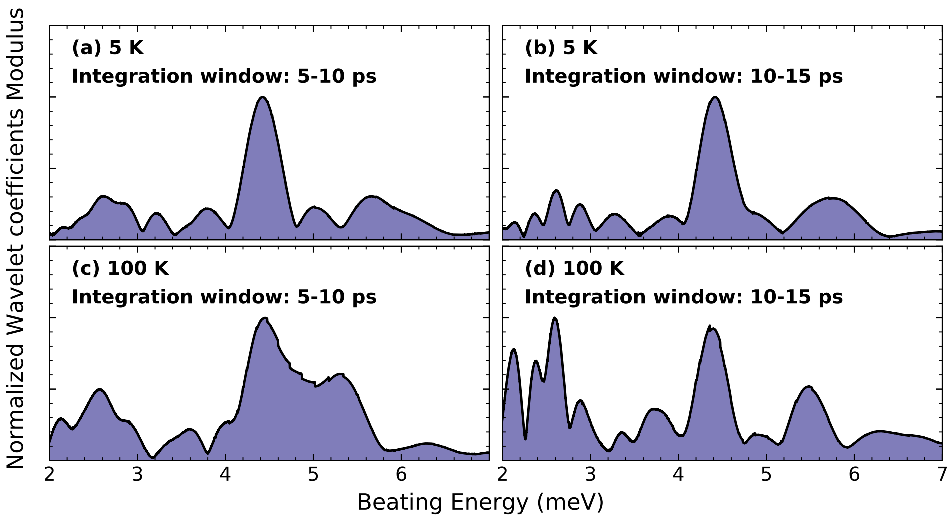

Figure S9: Time-integrated spectrum at 5 K between (a) 5-10 ps, (b) 10-15 ps and at 100 K between (c) 5-10 ps and (d) 10-15 ps.

4 Estimation of the dephasing rate

The coherence lifetime was extracted from M2 by fitting the data to a single exponential, as it is shown in Fig. S11. The error bars were determined with the confidence interval function at 99% using the python lmfit package. The traces for M1 did not follow a single exponential trend, then the decay rate was estimated as the value at which the amplitude is $1/e$ of the original amplitude, and the error bars were estimated as the time at which the amplitude is $1/e \pm 0.2$ of the original.

The dephasing rate is defined by equation S5, where Γ_0 is the dephasing rate in ps^{-1}:

$$\Gamma_0 = \frac{2}{\tau_{rate}}. \tag{S5}$$

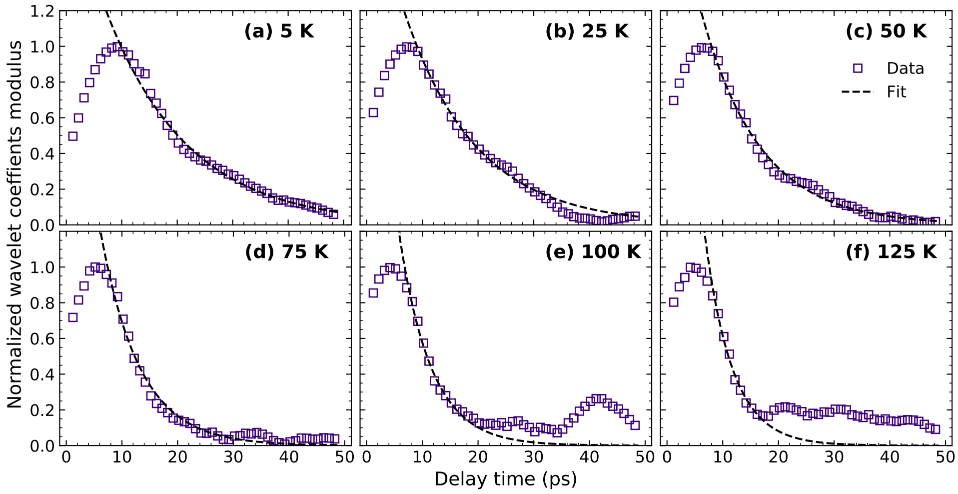

Figure S10: Dephasing rate extraction via an exponential fit of the energy cuts at 4.40 meV for the temperatures (a) 5 K, (b) 25 K, (c) 50 K, (d) 75 K, (e) 100 K and (f) 125 K.

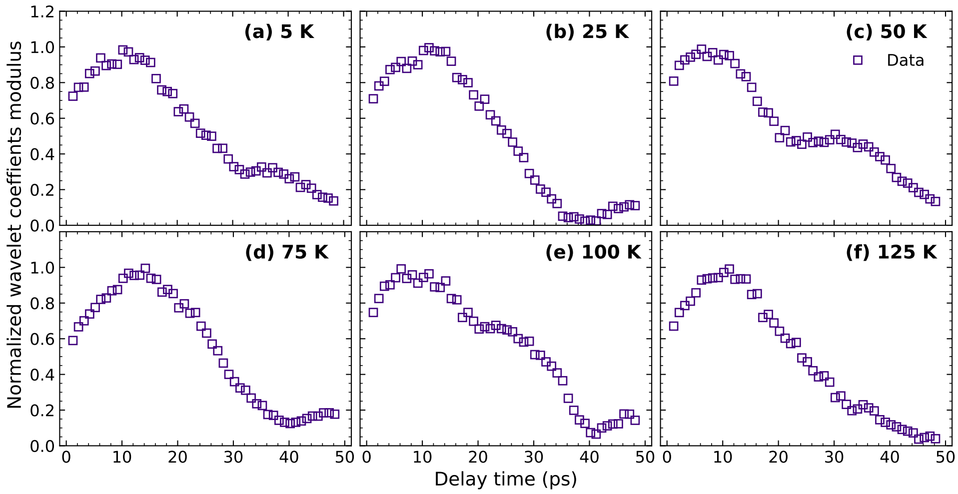

Figure S11: Energy cuts at 2.61 meV for the temperatures (a) 5 K, (b) 25 K, (c) 50 K, (d) 75 K, (e) 100 K and (f) 125 K.